

Full Paper

Pharmacokinetic Profile of Atenolol Aspirinate

Ana C. Montes-Gil¹, Marcos Zanfolin³, Cristina E. Okuyama¹, Sergio Lilla⁴, Delma P. Alves³, Vincenzo Santagada², Elisa Perissutti², Antonio Lavecchia², Ferdinando Fiorino², Beatrice Severino², Giuseppe Caliendo², Fernanda B. M. Priviero¹, Gustavo D. Mendes⁴, Jose L. Donato¹, Gilberto de Nucci¹

¹ Department of Pharmacology, Faculty of Medical Sciences, State University of Campinas, Campinas, São Paulo, Brazil

² Department of Pharmaceutical Chemistry, University of Naples "Federico II", Naples, Italy

³ CEMIB -Multidisciplinary Center for Biological Investigation. State University of Campinas, Campinas, São Paulo, Brazil

⁴ Galeno Research Unit, Campinas, São Paulo, Brazil

We report microwave-assisted synthetic routes, the pharmacokinetic profile along with results from ulcerogenicity and mutagenicity studies of atenolol aspirinate, and an already described derivative, in which acetyl salicylic acid (aspirin®) was connected to atenolol by an ester linkage. Atenolol aspirinate was stable towards aqueous hydrolysis but rapidly hydrolyzed in plasma ($t_{1/2}$ = 7.6 min). The results showed that the rapid and complete hydrolysis generates atenolol salicylate, which assumes a conformation stabilized by two intramolecular H-bonds, avoiding its further hydrolysis to salicylic acid and atenolol.

Keywords: Antihypertensive therapy / Atenolol / Microwave synthesis / Pharmacokinetics / Prodrug

Received: April 4, 2007; accepted: May 30, 2007

DOI 10.1002/ardp.200700070

Introduction

Atenolol antihypertensive therapy combined with acetyl salicylic acid is effective in reducing cardiovascular death, stroke, and myocardial infarction (MI) [1, 2]. Atenolol is a selective β_1 -adrenoceptor antagonist that is widely used to treat a wide range of cardiovascular disorders, including mild to moderate hypertension, angina pectoris and supraventricular arrhythmias, and arrhythmia prophylaxis after acute MI [3, 4]. Clinical trials have subsequently demonstrated that acetyl salicylic acid is

effective for both primary and secondary prevention of MI, stroke and cardiovascular death [5, 6], and in the acute management of MI, unstable angina, and embolic stroke [7–9]. Acetyl salicylic acid imparts its primary antithrombotic effects through the irreversible inhibition of platelet cyclooxygenase-1 (COX-1), thus preventing the formation of thromboxane A₂ (TXA₂) [10], potent aggregating, and vasoconstrictor molecules [11, 12]. The synthesis of isosorbide-based acetyl salicylic acid prodrugs with effective biological activity [13] has been previously reported.

In this work, we report a very detailed evaluation of the *in-vitro* and *in-vivo* activity, metabolic and pharmacokinetic profile along with results from ulcerogenicity and mutagenicity studies for atenolol aspirinate (ATA), an already described derivative in which acetyl salicylic acid (aspirin®) was joined to atenolol by an ester linkage [14, 15]. This derivative was designed on the basis of the prodrug strategy of coupling acetyl salicylic acid to frequently co-prescribed cardiovascular agents. ATA could act as a potential parallel mutual prodrug of both acetyl salicylic acid and atenolol enhancing their bioavailabil-

Correspondence: Gilberto de Nucci, 415 Jesuino Marcondes Machado Ave. 13092320 Campinas, SP, Brazil.

E-mail: denucci@dglnet.com.br

Fax: +55 19 3242-7439

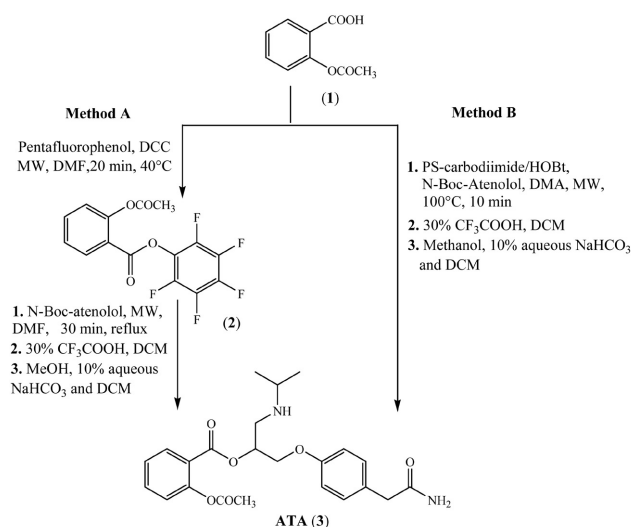
Abbreviations: Atenolol aspirinate (ATA); atenolol salicylate (ATS); carbonyldimidazole (CDI); cyclooxygenase-1 (COX-1); 1-benzotriazoleoxy (HOBt); benzotriazolyl-oxy tetramethyl uronium (HBTU); benzotriazolyl-oxy-tris-dimethylaminophosphonium (BOP); dicyclohexylcarbodiimide (DCC); *N,N*-dimethylformamide (DMF); isoproterenol (ISO); microwave-assisted organic synthesis (MAOS); myocardial infarction (MI); salicylic acid (SA); thromboxane A₂ (TXA₂); thromboxane B₂ (TXB₂)

ity and improving their therapeutic effects, as well as, reducing (due to a potential lower dosage) the risk of gastrointestinal bleeding and toxicity associated with acetyl salicylic acid. The large amount of ATA needed for these detailed pharmacological studies, prompted us to optimize and improve the synthetic route since the previously reported strategies (such as activation by DCC/DMAP, acid chloride formation, *etc.*) only allowed low yields (25–30%) [16]. Moreover, the ester linkage is present in a very large number of pharmacologically active compounds, therefore, the development of new procedures for the easy, clean, and racemization-free synthesis of ester is of topical interest in medicinal chemistry. On the basis of these considerations, ATA has been prepared employing microwave-assisted organic synthesis (MAOS) applied to two different esterification routes.

Results and discussion

Chemistry

In general, the formation of esters from alcohols and carboxylic acids implies the activation of the carboxy group by either the preventive conversion to a more reactive acylating agent, such as chloride, mixed anhydride, acyl azide, or active ester, or *in-situ* activation by using coupling reagents, such as dicyclohexylcarbodiimide (DCC), 1-benzotriazoleoxy (HOBT), benzotriazoloyloxy-trisdimethylaminophosphonium (BOP), carbonyldimidazole (CDI), or benzotriazoloyloxytetramethyluronium (HBTU). However, these methods have some drawbacks such as exothermic reaction, formation of byproducts, complicated conditions, and low selectivity. Microwave-assisted organic synthesis (MAOS) continues to affect synthetic chemistry significantly by enabling rapid, reproducible, and scalable chemistry development [16]. Numerous reactions including condensations, cycloadditions, heterocycle forming reactions, and metal-catalyzed cross-coupling have been explored under microwave conditions, some of which have been applied to medicinal chemistry [16, 17]. MAOS can facilitate the discovery of new reactions and reduce cycle time in optimization of reactions. As it relates to our efforts to develop efficient and robust methodologies and processes for high-throughput synthesis of pharmacologically interesting libraries for drug discovery, the exploration of microwave chemistry to access new compounds has been of particular interest to us [16]. Herein, we report, the pharmacological characterization and kinetic profile of ATA and two microwave-assisted approaches for the synthesis of ATA from readily available starting materials. In both methods, the process comprises the steps of a) protection of the atenolol secondary



Scheme 1. Synthetic route of 2-acetoxy-benzoic acid 2-(4-carbamoylmethyl-phenoxy)-1-(isopropylamino-methyl)-ethyl ester hydrochloride (ATA, 3).

dary amine group by forming a *N*-Boc derivative; b) activation of the carboxy group in acetyl salicylic acid and coupling with *N*-Boc-protected atenolol; c) removal of the protecting group from the atenolol secondary amine group.

In the first method, we applied microwave irradiation to the active pentafluorophenylester method (–OPfp, Scheme 1, Method A) for the activation of the carboxylic moiety, while in the second approach, microwave heating has been applied to a polymer-assisted solution-phase technique using the polymer-supported reagent PS-carbodiimide as dehydration agent in presence of HOBT (Scheme 1, Method B). In particular, in the first method, the final compound ATA was obtained as follows: acetyl salicylic acid 1 in anhydrous *N,N*-dimethylformamide (DMF) in presence of DCC was treated with pentafluorophenol to give the corresponding pentafluorophenyl ester derivative 2. Intermediate 2 was dissolved in DMF, *N*-Boc-atenolol was added, and the resulting solution was heated by microwave irradiation for 30 min. After work up, the intermediate *N*-Boc-atenolol-acetyl salicylic acid aspirinate was isolated by silica gel column chromatography (75% yield). Final compound ATA 3 was obtained by removal of the Boc-group with 30% trifluoroacetic acid (TFA) in dichloromethane (DCM) to give the corresponding trifluoroacetate salt that was dissolved in methanol, treated with 10% aqueous NaHCO₃ and extracted with dichloromethane. The solvent was evaporated and the residue was crystallized with diethyl ether.

In the second method, condensation between *N*-Boc-atenolol and acetyl salicylic acid 1 has been performed

applying microwave heating to a polymer-assisted solution-phase technique using polymer-supported reagent PS-carbodiimide as dehydration agent in the presence of HOBt and using *N,N*-dimethylacetamide (DMA) as solvent. The highly polar DMA ensured complete homogeneity (excluding the polymer-supported carbodiimide resin) and effective microwave heating of the reaction mixture. In this case, 10 min of irradiation was found sufficient to completely consume the starting acetyl salicylic acid **1** and the *N*-Boc-atenolol component from the reaction mixture, affording a clean conversion to the desired ester *N*-Boc-atenolol-aspirinate. Final compound **3** was obtained according to the first method.

Pharmacological results

Antiplatelet effects

Aggregation induced by arachidonic acid was used mainly to evaluate the effect of ATA on thromboxane-dependent platelet activation, since this metabolic pathway is inhibited by acetyl salicylic acid at very low concentrations [18]. ATA (30 μ M), unlike acetyl salicylic acid, had no inhibitory effect in all tested concentrations on AA-induced platelet aggregation and thromboxane A_2 (TXA₂) synthesis in platelets (thromboxane B₂ TXB₂: basal 1.98 ± 0.26 ng/mL, 845.81 ± 35.77 and 1.87 ± 0.75 ng/mL for 200 μ M of ATA and acetyl salicylic acid respectively, $p < 0.01$). *Ex-vivo* studies showed that ATA significantly inhibited serum-TXA₂ production at the highest doses administered, but was weaker than acetyl salicylic acid in both mice (at 0.28 mmol/kg (vehicle, 71.04 ± 17.8 ng/mL; 34.2 ± 11.2 and 4.3 ± 1.7 ng/mL of TXB₂ for ATA and acetyl salicylic acid, respectively, $p < 0.01$)) and rats (at 0.17 mmol/kg (vehicle, 216.9 ± 8.0 ng/mL; 70.3 ± 7.3 and 8.7 ± 1.1 ng/mL of TXB₂ for ATA and acetyl salicylic acid, respectively, $p < 0.05$)).

In-vitro β_1 -adrenoceptor-blocking effects on chronotropic responses in isolated rat right atria

Addition of ATA (0.1–10 μ M) to the bath had no effect on the basal rate (300 ± 11 and 315 ± 5 bpm (beats per minute));, before and after addition of ATA, respectively, at the highest concentration of 10 μ M). In contrast, addition of atenolol (0.1–10 μ M) provoked a significant reduction in the heart rate (270 ± 13 and 210 ± 10 bpm, before and after addition of atenolol, respectively, at the highest concentration of 10 μ M). Concentration-response curves to isoproterenol (ISO) in isolated rat right atria were obtained in the absence or presence of atenolol and ATA at concentrations of 0.1, 1 and 10 μ M. The potency (pEC_{50}) and maximal responses of ISO were not significantly unchanged by ATA 10 μ M (9.61 ± 0.17 and 135 ± 5.0 , respectively) in comparison to control animals

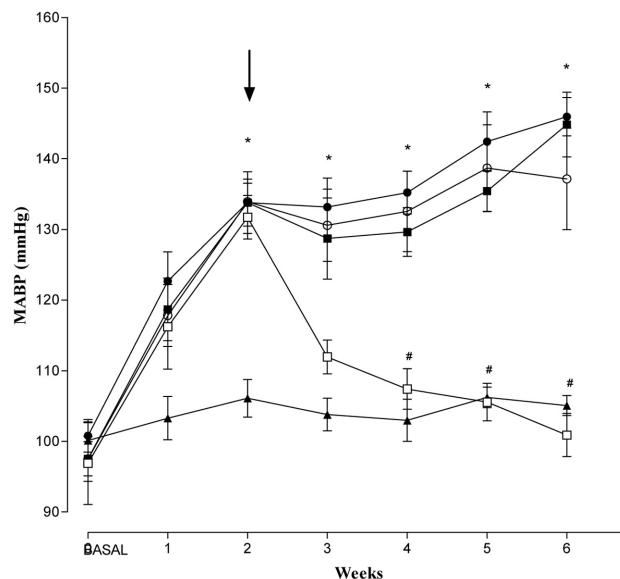


Figure 1. Effect of ATA on *N*^o-nitro-L-arginine methyl ester (L-NAME)-induced hypertension in rats. Mean Arterial Blood Pressure (MABP; mm Hg) was measured by radiotelemetry twice a week in Control (▲), L-NAME (●), L-NAME + ATA (○), L-NAME + atenolol (◻) and L-NAME + acetyl salicylic acid (■) groups ($n = 5$ to 8). The arrow shows beginning of concomitant treatment with the drugs, two weeks after L-NAME was initiated. Results are expressed as mean \pm SEM. * $p < 0.01$ compared to control group and # $p < 0.01$ compared to L-NAME group.

(9.93 ± 0.16 and 163 ± 21.75). As expected, atenolol addition caused a dose-dependent parallel shift to the right of the ISO concentration-response curves reducing significantly ($p < 0.05$) the pEC_{50} to ISO at concentrations of 1 and 10 μ M (8.09 ± 0.02 and 7.17 ± 0.02 , respectively) in comparison to control animals (9.38 ± 0.27).

Antihypertensive effect assessed by telemetry

Chronic administration of L-NAME (a non-selective NO-synthase antagonist) caused a significant increase in mean arterial blood pressure (Fig. 1). Atenolol treatment initiated two weeks after starting L-NAME administration, caused a significant reduction in the blood pressure (Fig. 1) and heart rate (302 ± 6 and 266 ± 4 bpm for L-NAME and L-NAME + atenolol-treated animals, respectively; values after four weeks of atenolol treatment). Treatment with either acetyl salicylic acid or ATA did not affect the hypertension or heart rate induced by chronic administration of L-NAME (Fig. 1).

Hydrolysis experiments

ATA was rapidly hydrolyzed ($t_{1/2} = 7.6$ min, $K_{obs} 9.1 \times 10^2$ min⁻¹) in dilute plasma solution. Hydrolysis was suppressed ($t_{1/2} = 421.5$ min, $K_{obs} 0.16 \times 10^2$ min⁻¹) when ATA

Table 1. Pseudo first-order rate constants and corresponding half-lives for the hydrolysis of atenolol aspirinate in aqueous solution at 37°C.

pH	2.5	7.4	9.4
k_{obs} ($\text{h}^{-1} \times 10^{-3}$)	12.27	27.85	108.0
$t_{1/2}$ (h)	56.47	24.88	6.41

was co-incubated with 3 μM of the esterase inhibitor neostigmine, suggesting that ATA plasma hydrolysis was presumably due to the presence of plasma pseudocholinesterase. Accurate mass measurement of the ATA hydrolysis product using a Q-TOF mass spectrometer showed that it was formed by deacetylation of ATA and corresponded to atenolol salicylate (ATS). The hydrolysis of ATA in aqueous solution at 37°C over the pH range 2.5–9.4, followed pseudo-first order kinetics over several half-life periods. Pseudo-first order plots for the decomposition of ATA were constructed from the logarithm of the remaining ester *versus* time. The pseudo first-order constants (k_{obs}) obtained and the half-lives are shown in Table 1. ATA exhibited high aqueous stability at all pH values; at the low pH 2.5 the half-life was 56.5 h. ATA aqueous stability is in agreement with the observation that most esters of acetyl salicylic acid generally exhibit higher aqueous stability than acetyl salicylic acid itself [19] because esterification masks the carboxylate, which performs an autocatalytic role in acetyl salicylic acid hydrolysis [20].

In-vitro metabolism

The kinetics of ATA microsomal metabolism determined by peak area of the drug and its unknown metabolites at different incubation times (Fig. 2) indicated that ATA undergoes an immediate and complete biotransformation generating three metabolites: M1 was formed within the first 5 min, then it was metabolized to the other unknown minor metabolic species M2 and M3, whose formation was time-dependent and parallel to the kinetics of M1 consumption. Accurate mass measurement of ATA metabolites using a Q-TOF mass spectrometer showed for M1 an accurate mass of 387.1905 Da (elemental composition of $\text{C}_{21}\text{H}_{26}\text{N}_2\text{O}_5$; error: 3.8 ppm with respect to the theoretical monoisotopic mass of 387.1920 Da), this molecular formula matched with that of ATS determined as the main hydrolysis product of ATA. The resulting spectra obtained by MS/MS analysis of M1 (Fig. 3) showed the same intense signal seen in the hydrolysis experiment that corresponded to the molecular mass of atenolol (m/z 267.1689). This confirmed that ATS is the main metabolite formed after *in-vitro* hepatic metabolism. Concerning M2 and M3 (as shown in Fig. 4)

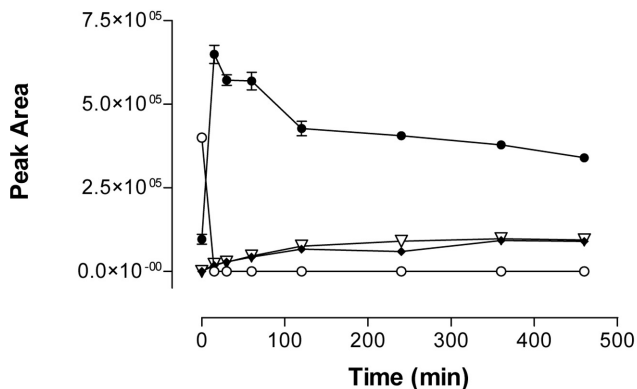


Figure 2. Kinetics of atenolol aspirinate (O) metabolism by rat-liver microsomes, three unknown metabolites were formed M1 (●), M2 (▽), and M3 (◆). Results are expressed as mean \pm SEM for three experiments.

their nominal masses were m/z 403 and the accurate masses of these compounds were determined to be m/z 403.1880 (M2) and m/z 403.1887 (M3). The mass shift for each metabolite was 16 Da relative to atenolol salicylate, suggesting the formation of monooxygenated metabolites with elemental composition of $\text{C}_{21}\text{H}_{26}\text{N}_2\text{O}_6$ (theoretical monoisotopic mass 403.1875 Da; error -2.7 ppm for M2 and -4.4 ppm for M3). A regenerating system of nicotinamide adenine dinucleotide phosphate (NADP⁺) was present during the incubation; oxidation products were therefore expected [21]. The MS/MS resulting spectra of M2 showed an important fragment at m/z 283.16 which would correspond to molecular mass of hydroxy atenolol, oxidation would have taken place at the acetamide group (atenolol subunit). Tandem MS spectra of M3 showed a signal only at m/z 267.17, demonstrating that this metabolite was probably oxidized at the benzene ring of the salicylic acid subunit, because the atenolol subunit was kept intact as it is shown in Fig. 4. The oxidation positions proposed for these metabolites were considered on the basis of mass fragments obtained after MS/MS analysis, and the literature metabolic oxidation pathways available for salicylic acid [22] and atenolol [23].

Pharmacokinetics after intravenous administration

Under our experimental conditions, acetyl salicylic acid was not detectable in any plasma sample taken from treated dogs; thus, for salicylate quantification in acetyl salicylic acid- or ATA-treated groups, the focus of the determination was concentrated on salicylic acid (SA) levels and kinetics, since acetyl salicylic acid and ATA are rapidly hydrolyzed in the plasma as indicated by the short half-lives of acetyl salicylic acid observed in humans [24] and dogs [25] in concert with our ATA

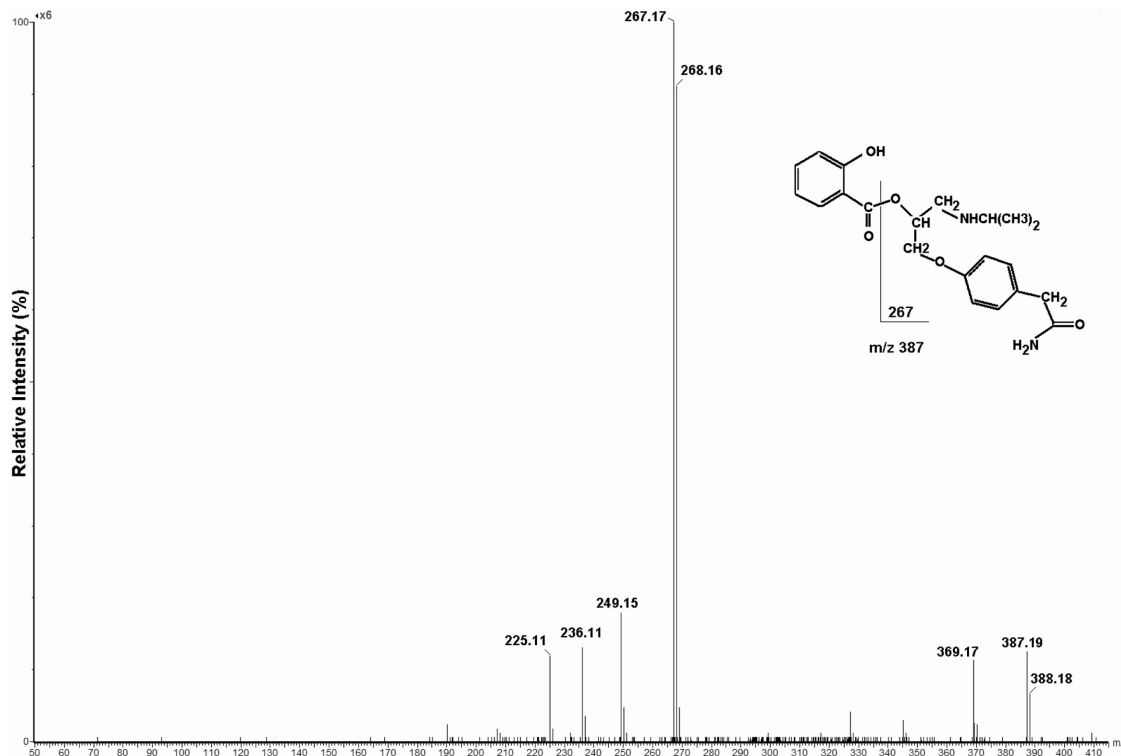


Figure 3. MS/MS product ion spectra and the predominant fragmentation pattern of M1. Atenolol salicylate was formed as a result of atenolol aspirinate deacetylation.

Table 2. Pharmacokinetic parameters of atenolol salicylate, atenolol, and salicylic acid following intravenous administration of atenolol aspirinate, acetyl salicylic acid, or atenolol.

Kinetic Parameter	Salicylic Acid		Atenolol		ATS
	ATA group	Acetyl salicylic acid group	ATA group	Acetyl salicylic acid group	ATA group
C_0 ($\mu\text{g/L}$)	$132.6 \pm 60.1^{\text{a}}$	5098.7 ± 444.4	$329.5 \pm 61.5^{\text{b}}$	6272.0 ± 4031	7583.1 ± 2154.2
$AUC_{0-24\text{h}}$ ($\mu\text{gh/L}$)	$110.9 \pm 82.9^{\text{c}}$	15182.6 ± 7100	$137.4 \pm 23.5^{\text{b}}$	8724.0 ± 1107	2849.0 ± 405.2
$AUC_{0-\infty}$ ($\mu\text{gh/L}$)	$159.4 \pm 85.6^{\text{c}}$	15366.8 ± 5806	$145.4 \pm 24.4^{\text{b}}$	8847.0 ± 1342	3163.9 ± 520.1
$T_{1/2}$ (h)	0.8 ± 0.3	1.7 ± 0.6	$1.3 \pm 0.8^{\text{b}}$	5.0 ± 0.2	8.2 ± 3.6
K_e (L/h)	0.9 ± 0.3	0.4 ± 0.2	0.6 ± 0.3	0.1 ± 0.01	0.1 ± 0.1
Vd (L/kg)	$42.6 \pm 18.4^{\text{a}}$	0.4 ± 0.04	$59.4 \pm 24.0^{\text{b}}$	2.5 ± 0.3	1.6 ± 0.3

Atenolol aspirinate (ATA), Atenolol salicylate (ATS). Data are expressed as mean \pm SD ($n = 3$).

^{a)} $p < 0.01$.

^{b)} $p < 0.05$ when compared with the acetyl salicylic acid group.

^{c)} $p < 0.01$ when compared with the atenolol group.

plasma hydrolysis results. Similarly, concentrations of ATS instead ATA were found in the dog plasma samples. The mean plasma concentration time profiles and the pharmacokinetic parameters for SA, atenolol, and ATS after *i.v.* administration of ATA, acetyl salicylic acid, or atenolol are shown in Fig. 5 and Table 2. The SA $AUC_{0-24\text{h}}$ for the ATA-treated dogs was 0.7% of that for the acetyl salicylic acid-treated dogs and the atenolol $AUC_{0-24\text{h}}$ for

the ATA-treated dogs was 1.6% of that for the atenolol-treated dogs. Plasma concentrations found for SA and atenolol in the ATA-treated group showed that both compounds originated from cleavage of ATS molecule at the benzoate ester linkage, generating concentration levels to a lesser extent than levels found after treatment with equimolar doses of the individual drugs.

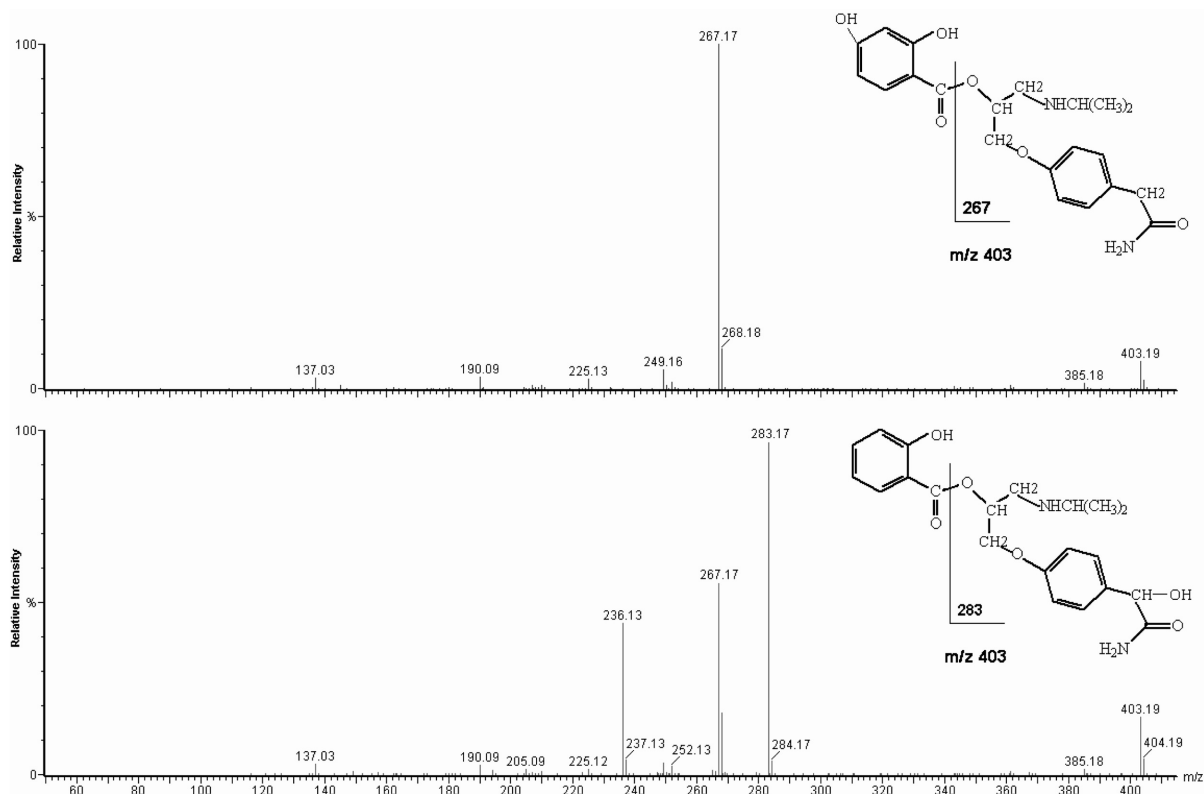


Figure 4. MS/MS product ion spectra and the predominant fragmentation patterns of the hydroxylated metabolites of atenolol salicylate, M2 (bottom panel) and M3 (top panel).

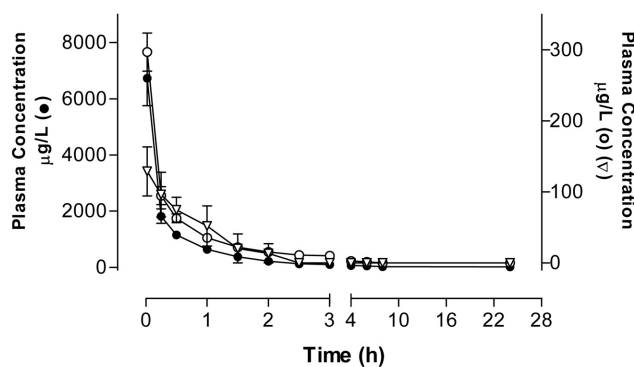


Figure 5. Mean plasma concentrations (\pm SEM) quantified for atenolol (\bullet), salicylic acid (∇), and atenolol salicylate (\circ) in dogs ($n = 3$) after intravenous administration (*bolus*) of atenolol aspirinate.

Mutagenicity assay (Ames Test)

ATA failed to elicit a positive mutagenic response in the Ames test after direct testing or in the presence of S9 mix in *Salmonella thyphimurium* strains TA98, TA 100, TA102, TA1535 and TA1537.

Gastric mucosal damage

ATA was significantly less ulcerogenic (0.66 mmol/kg) than acetyl salicylic acid after a single equimolar administration to rats. Gastric damage characterized by oedema associated with extensive gastric swelling, necrosis, and hemorrhage was confirmed by light microscopic examination of these tissues. Extensive gastric damage was also noted visually and microscopically after four weeks of oral treatment with 0.37 mmol/kg acetyl salicylic acid; there was a remarkable and significant difference ($p < 0.01$) between the “lesion index” values for acetyl salicylic acid and equivalent amounts of ATA (Fig. 6).

Conclusions

Our results showed that the coupling of atenolol and acetyl salicylic acid by means of an ester linkage did not produce good pharmacological results, neither *in vitro* nor *in vivo*. The coupling of acetyl salicylic acid abolished the *in vitro* blocking activity of the atenolol moiety, as shown by lacking the effect of ATA in the isolated atria prepara-

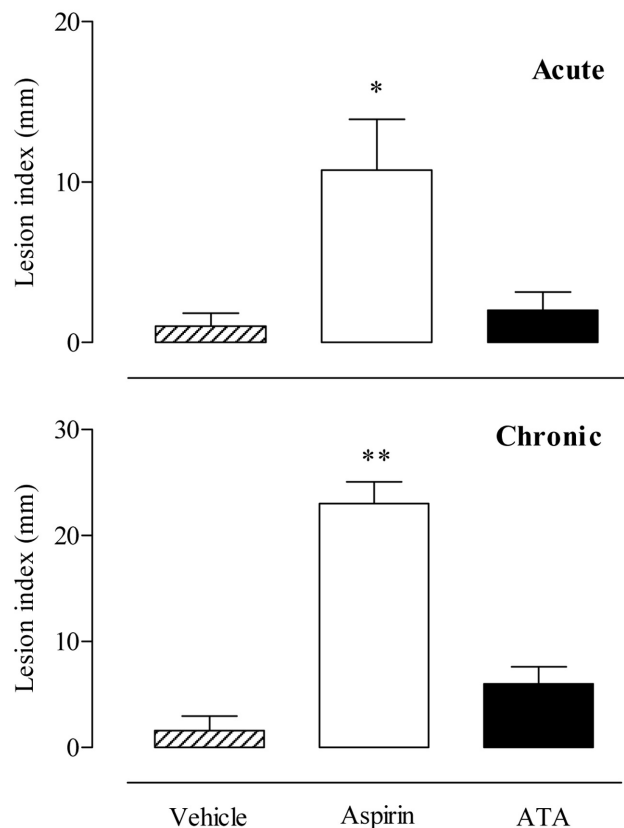


Figure 6. Gastric mucosal damage produced by oral administration of ATA or equivalent amounts of acetyl salicylic acid (0.37 or 0.66 mmol/kg, chronic or acute treatment, respectively). Mean \pm SEM ($n = 5$) * $p < 0.05$ and ** $p < 0.01$ compared to vehicle and ATA group.

tion. The L-NAME-induced hypertension is an established chronic model for evaluating antihypertensive agents [26] and atenolol has an important antihypertensive effect [27]. However, chronic administration of ATA by

the oral route did not exhibit any antihypertensive effect in this particular model, indicating that no release of atenolol *in vivo* was observed. The most likely explanation is that ATA was metabolized *in vivo* to ATS, and this complex made it difficult for plasma esterases to break the linkage between the salicylate and the atenolol. To inspect the different accessibility of the two ester branches of ATA to the hydrolytic attack of esterases, a conformational analysis was carried out by varying all torsions in the random search option of the SYBYL program (see Experimental, Section 4.12 for operational details). Interestingly, among the lowest energy conformers of ATA, a recurring feature was found: the presence of an intramolecular H-bond between the protonated nitrogen atom of the isopropyl-amino-methyl group and the ether oxygen of the phenyl-acetamide moiety so to form a 6-membered ring (Fig. 7). Consequently, the linkage between the salicylate and atenolol seems to be less accessible to the attack of the plasma esterases, being protected by the bulky aminoalkyl chain. On the other hand, the acetate group, lying in an exposed and unprotected position, is more prone to the attack by the esterases. Furthermore, when the hydrolysis of the acetate occurs, the free phenolic group of ATS is in turn engaged in an additional intramolecular H-bond with the salicylate carbonyl oxygen (Fig. 8). This peculiar conformation increases the thermodynamic stability of the molecule, thus justifying the low metabolic reactivity of ATS. ATA showed a safe gastric profile, as compared to acetyl salicylic acid. Probably, the linkage also made it difficult for acetyl salicylic acid to bind to the cyclooxygenase. This was corroborated by the lack of inhibition on TXA_2 synthesis, either in human platelets *in vitro*, but also in the *ex-vivo* evaluation made in mice and rats. Concerning the synthetic procedure, we have developed two microwave-enhanced, rapid and efficient methods for the synthesis

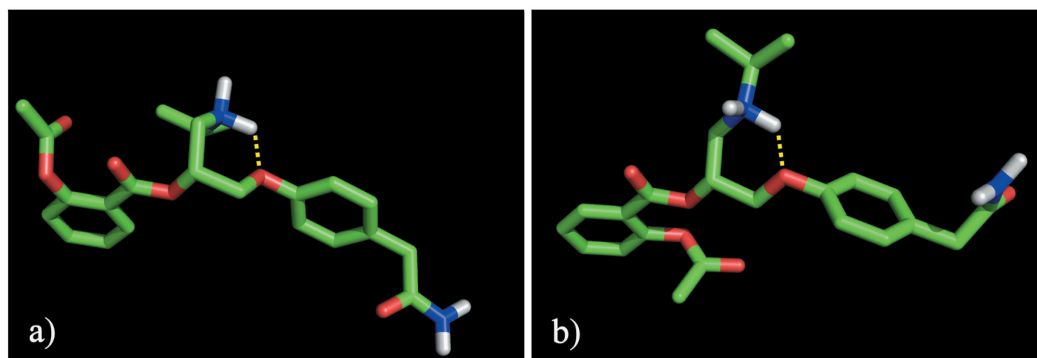


Figure 7. 3-D representation of the two lowest energy conformers of ATA (a and b). H-bonds are shown as dashed yellow lines. Non-polar hydrogens are omitted for clarity.

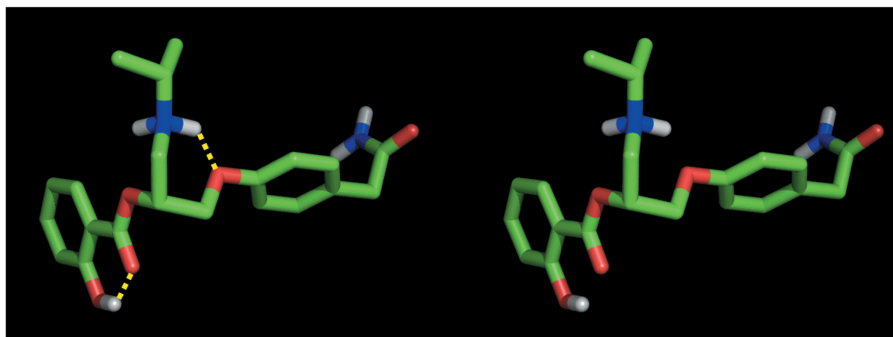


Figure 8. Stereoview showing the lowest energy conformer of atenolol salicylate (ATS). H-bonds are shown as dashed yellow lines. Non-polar hydrogens are omitted for clarity.

of ATA. One method uses readily available solid-phase reagent that not only results in higher yield but also greatly simplifies the purification process. Additionally, the use of microwave technology allowed us to quickly identify optimal reaction conditions with reaction times reduced from hours to minutes.

We thank Fundação de Amparo à Pesquisa do Estado de São Paulo (FAPESP) for the financial support.

Experimental

General procedures

Some synthetic steps were performed using a microwave oven ETHOS 1600 (Milestone, Sorisole, Italy) and a predefined microwave program composed of appropriate temperature (fiber optic temperature measurement), ramping, and holding steps. All microwave reactions were carried out in standard Pyrex glassware with a reflux condenser fitted through the roof of the microwave cavity. All reactions were followed by thin-layer chromatography (TLC) carried out on precoated silica gel plates Kieselgel⁶⁰F254 (E. Merck, A.G., Darmstadt, Germany) with diethyl ether/hexane (7 : 3, v/v) as solvent system. Visualization was accomplished with UV light. Chemical reagents and solvents were purchased from Aldrich Chemical Co and Carlo Erba Reagents (Rodano, Italy) and were used without further purification. ¹H-NMR, FTIR, and MS spectra were obtained on a Bruker AMX-500, Bruker IFS48 (Bruker Bioscience, Billerica, MA, USA), and LCQ ThermoQuest instruments (ThermoQuest CO, San Jose, CA, USA), respectively.

[3-(4-Carbamoylmethyl-phenoxy)-2-hydroxy-propyl]-isopropyl-carbamic acid tert-butyl ester (N-Boc-atenolol)

A solution of di-*tert*-butyldicarbonate (0.75 g, 3.44 mmol) in *t*-BuOH (3.5 mL) was added over 30 min to a solution of atenolol (0.82 g, 3.1 mmol) in a mixture of *t*-BuOH (3.5 mL) and distilled H₂O (3.5 mL), and the mixture was stirred for 3 h at room temperature. Then, the solution was poured into distilled water and extracted with diethyl ether (4 × 10 mL). The combined organic layers were washed with saturated NaCl solution (3 × 10 mL) and then dried over anhydrous MgSO₄. The mixture was filtered and

the filtrate was concentrated *in vacuo* to obtain 1.25 g of crude *N*-Boc-atenolol. Further purification was performed by chromatography on silica gel using diethyl ether as eluent to give the final product *N*-Boc-atenolol as an almost colorless oil (yield: 1.07 g, 95%).

2-Acetoxy-benzoic acid pentafluorophenyl ester 2

A solution of acetyl salicylic acid **1** (1 g, 5.5 mmol) in anhydrous DMF (20 mL) was treated with pentafluorophenol (1.02 g, 5.5 mmol) in the presence of DCC (1.2 g, 6.0 mmol) at 40 °C for 20 min by microwave heating (300 W). After removal of the precipitated urea by filtration and DMF under reduced pressure, the reaction mixture was dissolved in ethyl acetate, followed by removal of more dicyclohexylurea. The solvent was removed under reduced pressure and the residual oil was crystallized from ethanol, to give the 2-acetoxy-benzoic acid pentafluorophenyl ester derivative **2** (yield: 1.78 g, 95%; mp: 94–95 °C) ¹H-NMR (CDCl₃): δ H (selected peaks only) 2.31 (3H, s, OCOCH₃), 7.20, 7.40, 7.68; and 8.21 (4H, d, t, t, d, acetyl salicylic acid, aromatic proton resonances).

2-Acetoxy-benzoic acid 2-(4-carbamoylmethyl-phenoxy)-1-(isopropylamino-methyl)-ethyl ester (ATA, 3)

Method A: The pentafluorophenyl ester derivative **2** (415 mg, 1.2 mmol) was dissolved in DMF (80 mL) and to this solution was added *N*-Boc-atenolol (1.74 g, 4.8 mmol, 4 eq). After 30 min while refluxing on microwave irradiation (300 W), TLC showed the formation of the desired ester *N*-Boc-atenolol-aspirinate. Evaporation of the solvent on the rotary evaporator left a gum, which was dissolved in DCM and passed through a plug of silica, eluting with ethyl acetate, to give *N*-Boc-atenolol-aspirinate as an oil (yield: 475 mg, 75%). ¹H-NMR (CDCl₃): δ H selected peak only) 2.32 (3H, s, CH₃COO). *N*-Boc-atenolol-aspirinate (324 mg, 0.6 mmol) was added to a stirred solution of TFA (6 mL) in anhydrous DCM (6 mL) at room temperature. After 1 h of stirring, the solvent was removed by evaporation under reduced pressure, to leave the alkylammonium trifluoroacetate salt derivative as a clear colorless oil (yield: 300 mg, 92%). ¹H-NMR (CDCl₃): δ H selected peaks only) 1.33 (6H, m, CH(CH₃)₂), 2.29 (3H, s, CH₃COO), 3.44 (2H, s, PhCH₂CONH₂), 3.49 and 4.23 (5H, m, OCH₂CH₂NCH), 5.53, 5.60, and 6.66 (3H, br, m, CH-OCO and CONH₂), 6.85 and 7.08 (4H, 2d, benzeneacetamide proton resonances), 7.09, 7.28, 7.57, and 7.99 (4H, d, t, t, d, aspirin aromatic proton resonances). ¹³C-NMR (CDCl₃): δ C (selected peaks only) 19.0 (2 × C, CH(CH₃)₂), 21.4 (1 × C,

CH₃CO-O), 42.2 (1C, PhCH₂CONH₂), 55.0 and 70.1 (2 × C, CHCH₂NCH(CH₃)₂, 67.7 and 71.9 (2C, -NCH₂-CHCH₂OAr), 115 and 132 (2 × C, benzeneacetamide CH resonances), 124, 128, 134, and 136 (4 × C, acetyl salicylic acid aromatic CH resonances), 122, 130, 152, and 157 (4 × C, quaternary aromatic carbons), 157, 164, and 172 (3 × C, COO, COO and CONH₂). ATA · TFA (0.8 g) was dissolved in 10 mL of methanol and treated with 10% aqueous NaHCO₃ (150 mL). The aqueous solution was extracted with DCM (3 × 50 mL). The organic solution was dried on Na₂SO₄ and evaporated yielding ATA that was crystallized from diethyl ether (yield: 568 mg, 90%).

2-Acetoxy-benzoic acid 2-(4-carbamoylmethyl-phenoxy)-1-(isopropylamino-methyl)-ethyl ester (ATA, 3)

Method B: PS-Carbodiimide resin (1 g, 1.2 mmol) was charged in a two-necked flask. To the resin were added acetyl salicylic acid (108 mg, 0.6 mmol) in DMA (5 mL), HOBt (81 mg, 0.6 mmol) in DMA (5 mL) and *N*-Boc-atenolol (220 mg, 0.6 mmol) in DMA. The mixture was heated by microwave irradiation at 100°C (300 W) for 10 min. After cooling, the reaction mixture was diluted with 10 mL methanol and transferred to a pre-packed column of Si-Carbonate (5 g, 0.7 mmol/g), which had been previously conditioned with methanol and the eluent collected via gravity filtration. The column was washed with methanol (2 × 15 mL) and the solvent evaporated at reduced pressure to afford crude *N*-Boc-atenolol-aspirinate which was purified on a silica gel column eluted with ethyl acetate to give pure *N*-Boc-atenolol-aspirinate as an oil (yield: 285 mg, 90%). Finally, ATA 3 was obtained as previously described in the method A.

Platelet aggregation

Venous blood samples were collected from five human adult, healthy volunteers, who had not taken any medication drug for at least two weeks. Platelet-rich plasma (PRP) was prepared by low-speed centrifugation of 10 mL citrated blood at 200 g × 10 min at room temperature. Increasing amounts of ATA or acetyl salicylic acid (10 μM to 1 mM, dissolved in DMSO 10%) were incubated with 400 μL aliquots of PRP at 37°C for 5, 10, or 30 min before agonist arachidonic acid (AA) 1 mM addition. Aggregation was monitored for 5 min in a double-channel whole blood, Lumi-Aggregometer, (Chrono-log 560 CA; Chrono-log Corp., Haverton, PA, USA). The antiaggregatory activity of the drugs was evaluated as %-inhibition of platelet aggregation compared to control samples. At the end of the incubation period, PRP was collected in EDTA to stop aggregation; the tested platelets were centrifuged at 2000 g × 4 min. The supernatant was collected and stored at -20°C. Concentrations of TXB₂ (hydrolysis product of TXA₂) were determined by immunoenzymatic assay using a commercial kit (Cayman Chemical Co., Ann Arbor, MI, USA).

Thromboxane synthesis stimulated ex-vivo

Male Swiss mice weighing 25–30 g (n = 7) were treated orally with acetyl salicylic acid 0.06, 0.17, and 0.28 mmol/kg or the same doses of ATA dissolved in DMSO 10%. Additionally, male Wistar rats weighing 150–200 g (n = 5), received 0.17 mmol/kg of acetyl salicylic acid or the same doses of ATA. Three hours after drug administration, the animals were anesthetized with halothane and then blood samples were obtained by intracardiac puncture and transferred into glass tubes without anticoagulant and allowed to clot at 37°C for 60 min; serum was sepa-

rated by centrifugation (1000 g × 10 min) and kept at -20°C until assayed for TXB₂ by immunoenzymatic assay.

β₁-Adrenoceptor antagonist effects; isolated right atria and concentration response-curves

Right atria from male Wistar rats (200–300 g, n = 5) were isolated, processed, and data were evaluated according to our reported procedure [28]. Concentration–response curves for the chronotropic actions of isoproterenol (ISO 10 pM–1 mM) were obtained in the absence or in the presence of atenolol or ATA (0.1, 1.0, and 10 μM).

Antihypertensive effects

Male rats (Wistar-Uni specific pathogen free (SPF); 130–200 g) provided by the Central Animal House (CEMIB-UNICAMP) were maintained in individual cages under SPF, light and temperature-controlled conditions (12 h day / 12 h night, 25°C). The antihypertensive effects were assessed by telemetry, methodology was developed according to our reported procedure [29]. The animals were anaesthetized, surgically manipulated, and equipped with a radiotelemetry device into the descending aorta. Data acquisition was performed during 60 s twice a week for six consecutive weeks (Data Science Inc., St. Paul, MN, USA). The animals were initially divided into control (n = 5, received tap water alone) or L-NAME groups. Two weeks later, when the rats were hypertensive, concomitant treatment was initiated with 0.37 mmol/kg of ATA (n = 8) or equimolar doses of atenolol (n = 7), or acetyl salicylic acid (n = 6); five rats received L-NAME alone. L-NAME was dissolved in the drinking water and the daily dose was 20 mg/rat/day. Atenolol, acetyl salicylic acid and ATA were dissolved in 30% DMSO and administered by diary oral gavage (vol. 0.8 mL) during four weeks, L-NAME and control animals also received 30% DMSO.

Hydrolysis kinetics in human plasma and aqueous buffer solutions

The hydrolysis of ATA (initial concentration 0.2 mM) was studied in 0.01 M phosphate buffer of pH 7.4 containing 10% human plasma and aqueous buffer solutions of pH 2.5, 7.4, and 9.4 (acetate, phosphate, and borate buffers, 0.01 M respectively) using previously reported methodology [19]. Plasma hydrolysis was also performed in the presence of neostigmine (3 μM) to confirm the role of esterases in the hydrolysis of ATA. Analyses were performed in triplicate, using RP–HPLC. Eluted peaks were collected and introduced in a quadrupole time-of-flight mass spectrometer (QTOF-MS) source for accurate mass determination of hydrolysis products under our previously reported chromatographic and mass spectrometry conditions [30].

In-vitro hepatic metabolism

Rat liver microsomes were prepared following a standard procedure: tissues were homogenized in ice-cold 0.1 M potassium phosphate, pH 7.5, containing 0.15 M KCl and 0.1 mM EDTA (1 : 5 w/v). Crude homogenate was centrifuged at 12000 g for 20 min and the supernatant centrifuged at 105000 g for 60 min. The microsomal pellets were resuspended in buffer phosphate (0.2 M) containing 20% glycerol and frozen at -80°C. Protein contents (40.6 mg protein/mL) were estimated using the Lowry [31] method and cytochrome P-450 content (1.3 nmol/mg protein) was assayed according to the method of Omura and Sato

[32]. ATA was incubated with microsomes under the following conditions and final concentrations: ATA 50 μM , microsomal protein 1 mg/mL, NADPH-generating system (glucose 6-phosphate 10 mM, MgCl_2 10 mM, and glucose 6-phosphate dehydrogenase 2 U, 0.5 mM) and Tris-HCl buffer (pH 7.4; 0.072 M) in a total volume of 500 μL . After different incubation times at 37°C, reactions were terminated by adding ice-cold methanol and vortex-mixing. Separated supernatant aliquots (50 μL) were submitted to RP-HPLC analysis; chromatographic peaks obtained were manually collected and introduced in a QTOF-MS source for accurate mass measurement of ATA metabolites under our previously reported chromatographic and mass spectrometry conditions [30].

Pharmacokinetics after a single intravenous dose

ATA, atenolol, or acetyl salicylic acid at 11.2 $\mu\text{mol/kg}$ of body weight, were administered dissolved in 10% DMSO as a single intravenous (*i.v.*) bolus into the medial saphenous vein from the hind leg of male beagles weighing 10 to 15 kg ($n = 3$). Venous blood samples (3 mL) were collected immediately before and at 0.02 to 24 h after drug administration in heparinized and chilled tubes. Samples were then centrifuged at 2700 g for 10 min at 4°C. Plasma was aspirated off, chilled with liquid N, and stored at -20°C until analysis. For plasma extraction of atenolol, samples (100 μL) were spiked with the internal standard nadolol; 0.025 $\mu\text{g/mL}$, and then 50 μL of ammonium acetate (50%) were added to the sample and vortexed. Diethyl ether (4 mL) - DCM (60 : 40 v/v) was added for liquid-liquid extraction, centrifuged (3200 g for 1 min), frozen for 10 min, and after phase separation, the collected organic phases were evaporated to dryness under a nitrogen stream at 50°C, taken up in 100 μL of acetonitrile - water (10 : 90 v/v) - ammonium hydroxide (2.5 mM), vortexed and transferred to an autosampler vial. For acetyl salicylic acid and salicylic acid (SA) extraction, cinnamic acid 0.025 $\mu\text{g/mL}$ was used as an internal standard, formic acid (3%) was added to acidify the sample before liquid-liquid extraction with ether - hexane (80 : 20 v/v) and used instead ammonium hydroxide in the reconstitution solution.

LC-MS/MS analysis

The LC-MS/MS system comprised a liquid chromatograph Shimadzu model LC-10AVP (Shimadzu, Tokyo Japan); a degasser Agilent model G1322-A (Agilent, Palo Alto, CA, USA) and an auto-injector CTC analytics model HTS Pal (CTC Analytics, Zwingen, Switzerland); coupled to an Applied Biosystems Sciex API-2000 triple-quadrupole mass spectrometer equipped with an ESI source (Applied Biosystems, Foster City, CA, USA). The quadrupoles were operated with unit resolution in the positive ion mode (for ATA and atenolol) and negative ion mode (for acetyl salicylic acid and SA). An Alltech, Prevaal, C_{18} (5 μm , 150 \times 4.6 mm) column (Alltech, Deerfield, IL, USA) and mobile phase composed of acetonitrile - water (70 : 30 v/v) - ammonium acetate (10 mM) - acetic acid (16.7 mM) were used for atenolol analysis and acetonitrile - water (70 : 30 v/v) - formic acid (10 mM) for SA analysis. The run time was 5 min; quantification was performed with Masslynx software version 3.5 (Micromass, UK). Pharmacokinetic parameters were calculated using the software WinNonLin Professional Network Edition 1.5 (Pharsight Corp., Mountain View, CA, USA)

Gastric mucosal damage

The ability to produce gastric damage was evaluated according to reported procedures [33, 34]. Male Wistar rats ($n = 5$) weighing 180–200 g, were deprived of food but not of water 24 h before the experiment. Three hours after oral administration of the vehicle (DMSO 30%), acetyl salicylic acid 0.66 mmol/kg or an equivalent amount of ATA, rats were sacrificed and their stomachs were removed, opened along the lesser curvature and examined using magnifier lenses for the presence of macroscopically visible lesions. Each individual hemorrhagic lesion was measured along its greatest length (<1 mm = rating of 1; 1–2 mm = rating of 2; >2 mm = rating according to their length in mm). The overall total was designated as the “lesion index”. The stomachs were fixed in buffered formalin (pH 7.4) and processed by routine methods before mounting on glass slides and staining with hematoxylin and eosin. Coded slides (to avoid observer bias) were evaluated using a light microscope. Additionally, taking advantage of chronic treatment followed by telemetry protocol, we evaluated gastric lesions after four weeks oral treatment with 0.37 mmol/kg acetyl salicylic acid or equimolar doses of ATA.

Mutagenicity assay (Ames test)

Mutagenicity of ATA (31–500 $\mu\text{g/plate}$) dissolved in 30% DMSO was assessed in the Ames–Salmonella assay with strains TA98, TA100, TA102, TA1535, and TA1537 according to our previously reported method [35].

Molecular modeling

Molecular modeling calculations and graphics manipulations were performed on a Silicon Graphics Tezro workstation equipped with four 700 MHz R16000 processors using the SYBYL7.2 software package (Sybyl Molecular Modeling System Tripos Inc., St. Louis, MO, USA). The core structures of ATA and ATS were retrieved from Cambridge Structural Database (CSD) [36] and modified according the standard bond lengths and bond angles of the SYBYL fragment library with the TRIPOS force field [37]. The ligands were modelled in the R configuration. Geometric optimizations were carried out with the SYBYL/MAXI-MIN2 minimizer by applying the BFGS (Broyden, Fletcher, Goldfarb, and Shanon) algorithm [38] and setting a root-mean-squares (rms) gradient of the forces acting on each atom of 0.05 kcal/molÅ as the convergence criterion. A conformational analysis was performed on ATA and ATS by varying all torsions in the randomsearch option [39] of the SYBYL program. In this Monte Carlo-like method, many conformations are generated by randomly perturbing selected rotatable bonds and then the conformations are energy-minimized. Each new conformation is compared against all others found so far, to see if it is unique. Randomsearch was run under the following settings (reported in parentheses): a) the maximum number of hits, which defines the number of times each conformation must be found to stop the search for new conformations ($n = 6$); b) the rms threshold, which defines the maximum rms difference between two conformations before they are considered different (0.7 Å); c) the energy cut-off, which defines the maximum allowed energy for a conformation to be kept and energy-minimized ($E = \text{energy of the input conformer plus } 50 \text{ kcal/mol}$); d) the maximum number of attempts to find a new conformation (1000 for both compounds). Among the resulting conformations, only those associated with energy within 3 kcal/mol from the global minimum

(11 for ATA and 12 for ATS) were further minimized with MOPAC/AM1 [40] (default values; additional keywords MMOK and PRECISE). Only low-energy conformations (energy less than 3 kcal/mol above the absolute minimum energy) were investigated further.

Statistical analysis

Results are expressed as means \pm S.E.M or SD. Differences between controls and treatments were analyzed by using the Student's *t* test. A value $p=0.05$ was considered as statistically significant.

References

- [1] E. Fossum, A. Moan, S. E. Kjeldsen, R. B. Devereux, *et al.*, *J. Am. Coll. Cardiol.* **2005**, *46*, 770–775.
- [2] V. Hinstridge, T. M. Speight, *Drugs* **1991**, *42*, 8–20.
- [3] A. N. Wadworth, D. Murdoch, R. N. Brogden, *Drugs* **1991**, *42*, 468–510.
- [4] K. E. Ellison, G. Gandhi, *Drugs* **2005**, *65*, 787–797.
- [5] Steering Committee of the Physicians' Health Study Research Group. *N. Engl. J. Med.* **1989**, *321*, 129–135.
- [6] Antiplatelet Trialists' Collaboration, *BMJ* **1994**, *308*, 81–106.
- [7] Antithrombotic Trialists' Collaboration, *BMJ* **2002**, *324*, 71–86.
- [8] S. Yusuf, F. Zhao, S. R. Mehta, S. Chrolavicius, *et al.*, *N. Engl. J. Med.* **2001**, *345*, 494–502.
- [9] ISIS-2 (Second International Study of Infarct Survival) Collaborative Group. *Lancet* **1988**, *13*, 349–360.
- [10] M. Hamberg, J. Svensson, B. Samuelsson, *Proc. Natl. Acad. Sci. USA* **1975**, *72*, 2994–2998.
- [11] G. de Gaetano, *Haematologica* **2001**, *86*, 349–356.
- [12] P. J. Loll, D. Picot, R. M. Garavito, *Nature Struct. Biol.* **1995**, *2*, 637–643.
- [13] J. F. Gilmer, L. M. Moriarty, M. N. Lally, J. M. Clancy, *Eur. J. Pharm. Sci.* **2002**, *16*, 297–304.
- [14] W. Byrne, A. Rynne, *PCT Int. Appl.* WO9520568, **1995**.
- [15] W. Byrne, J. F. Gilmer, *PCT Int. Appl.* WO9705128, **1997**.
- [16] V. Santagada, E. Perissutti, G. Caliendo, *Curr. Med. Chem.* **2002**, *9*, 1251–1238; V. Santagada, F. Frecentese, E. Perissutti, L. Faretto, G. Caliendo, *QSAR Comb. Sci.* **2004**, *23*, 919–944.
- [17] O. C. Kappe, D. Dallinger, *Nat. Rev. Drug Discov.* **2006**, *5*, 51–63.
- [18] P. Minuz, C. Lechi, R. Tommasoli, S. Gaino, *et al.*, *Thromb. Res.* **1995**, *80*, 367–376.
- [19] N. M. Nielsen, H. Bundgaard, *J. Med. Chem.* **1989**, *32*, 727–734.
- [20] T. St Pierre, W. P. Jencks, *J. Am. Chem. Soc.* **1968**, *90*, 3817–3827.
- [21] P. R. Tiller, A. P. Land, I. Jardine, D. M. Murphy, *et al.*, *J. Chromatogr. A* **1998**, *794*, 15–25.
- [22] A. J. Hutt, J. Caldwell, R. L. Smith, *Xenobiotica* **1986**, *16*, 239–249.
- [23] P. R. Reeves, D. J. Barnfield, S. Longshaw, D. A. McIntosh, M. J. Winrow, *Xenobiotica* **1978**, *8*, 305–311.
- [24] D. J. Siebert, F. Bochner, D. M. Imhoff, S. Watts, *et al.*, *Clin. Pharmacol. Ther.* **1983**, *33*, 367–374.
- [25] D. J. Morton, D. C. Knottenbelt, *J. S. Afr. Vet. Assoc.* **1989**, *60*, 191–194.
- [26] M. O. Ribeiro, E. Antunes, G. de Nucci, S. M. Lovisolio, R. Zatz, *Hypertension* **1992**, *20*, 298–303.
- [27] S. R. Pacca, A. P. de Azevedo, C. F. de Oliveira, I. M. de Luca, *et al.*, *J. Cardiovasc. Pharmacol.* **2002**, *39*, 201–207.
- [28] S. R. Riado, A. Zanesco, L. A. Barker, I. M. De Luca, *et al.*, *Hypertension* **1999**, *34*, 802–807.
- [29] M. Zanfolin, R. Faro, E. G. Araujo, A. M. Guaraldo, *et al.*, *J. Cardiovasc. Pharmacol.* **2006**, *47*, 391–395.
- [30] B. Bicalho, G. C. Guzzo, S. Lilla, H. O. Dos Santos, *et al.*, *Curr. Drug Metab.* **2005**, *6*, 519–529.
- [31] O. H. Lowry, N. J. Rosebrough, A. L. Farr, R. I. Randall, *J. Biol. Chem.* **1951**, *193*, 265–275.
- [32] T. Omura, R. Sato, *J. Biol. Chem.* **1964**, *239*, 2370–2378.
- [33] C. Cena, M. L. Lolli, L. Lazzarato, E. Guaita, *et al.*, *J. Med. Chem.* **2003**, *46*, 747–754.
- [34] J. L. Wallace, M. N. Muscara, W. McKnight, M. Dickey, *et al.*, *Thromb. Res.* **1999**, *93*, 43–50.
- [35] H. S. Cardoso, B. Bicalho, P. Genari, V. Santagada, *et al.*, *Eur. J. Med. Chem.* **2006**, *41*, 408–416.
- [36] F. H. Allen, S. Bellard, M. D. Brice, B. A. Cartwright, *et al.*, *Acta Crystallogr.* **1979**, *B35*, 2331–2339.
- [37] J. G. Vinter, A. Davis, M. R. Saunders, *J. Comput-Aided Mol. Des.* **1987**, *1*, 31–51.
- [38] J. Head, M. C. Zerner, *Chem. Phys. Lett.* **1985**, *122*, 264–270.
- [39] A. M. Treasurywala, E. P. Jaeger, M. L. Peterson, *J. Comput. Chem.* **1996**, *17*, 1171–1182.
- [40] MOPAC (version 6.0) is available from Quantum Chemistry Program Exchange, No. 455; M. J. S. Dewar, E. G. Zebisch, E. F. Healy, J. J. P. Stewart, *J. Am. Chem. Soc.* **1985**, *107*, 3902–3909.